

Photodissociation of propyne and allene at 193 nm with vacuum ultraviolet detection of the products

Chi-Kung Ni,^{a)} J. D. Huang,^{b)} Yit Tsong Chen,^{b)} A. H. Kung, and W. M. Jackson^{c)}
*Institute of Atomic and Molecular Science, Academia Sinica,
Taipei, P.O. Box 23-166, Taiwan, Republic of China*

(Received 5 October 1998; accepted 10 November 1998)

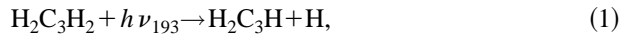
Vacuum ultraviolet (VUV) laser photoionization is combined with time-of-flight (TOF) mass spectrometry to determine the photofragments produced from the laser photodissociation of allene and propyne in a molecular beam. Detection of $C_3H_3^+$ confirms that atomic hydrogen elimination is the primary process for both of these molecules. A hydrogen molecule elimination channel and a low mass carbon fragmentation channel of allene to produce $C_3H_2 + H_2$ and $CH_2 + C_2H_2$, respectively, have also been identified. Different ratios of various dissociation channels from these two molecules suggest that the dissociation mechanisms of these two isomers are different. Dissociation must occur before complete isomerization. These results are discussed in terms of recent theoretical calculations on the ground and excited states of these molecules. Secondary photodissociation of the products has been observed, even though the laser energies that have been used are less than 8 mJ/cm² and the photolysis laser is not focused. Therefore, the present results show how important it is to determine product distributions as a function of the laser energy.

© 1999 American Institute of Physics. [S0021-9606(99)00807-7]

INTRODUCTION

In recent years, there have been many efforts to understand the photodissociation dynamics of allene and propyne.^{1–10} One of the reasons is that C_3H_4 is the smallest hydrocarbon with geometrical isomers. Very good *ab initio* calculations show there are many pathways on the ground state surface that can convert the molecule from allene to cyclopropene and propyne.^{11–15} The mechanisms for the interconversions of allene and propyne involve H atom migration (1,3 as well as 1,2) and ring closure. Thus, this system is the prototypical example of many of the most important reactions in organic chemistry. Theoretical calculations show the largest activation barrier between these isomers is less than 66 kcal/mol, but this is significantly lower than the minimum energy of 87.8 kcal/mol required for dissociation from the ground electronic state. There is therefore a distinct possibility for extensive isomerization prior to dissociation of the molecule.

Earlier experimental and theoretical work on the photolysis of allene at 193 nm showed that this molecule undergoes internal conversion to the ground state surface before dissociation.^{1–4} Both H atom and H_2 elimination were observed at this wavelength, and relative yields of 0.89 and 0.11, respectively, were measured for the following two reactions:



These channels were identified and characterized using photofragment translational spectroscopy to identify the products and determine their recoil velocities.¹ No evidence for carbon bond breakage was observed in this study.

The photolysis of propyne has also been studied recently by Satyapal and Bersohn⁹ and Seki and Okabe.¹⁰ In the Bersohn work, CH_3C_2D was photolyzed and VUV laser fluorescence detection was used to show that only D atoms are formed when the molecule is photolyzed at 193 nm.⁹ Seki and Okabe used product analysis to derive quantum yields at 193 nm for reaction 3 of 0.7 ± 0.1 and for reaction 4 of 0.11 ± 0.01 .¹⁰ They also agreed that the H atom comes only from the acetylenic hydrogen,



An issue in the photodissociation of these two molecules is whether the dissociation channels are the same for both of them. If the relative abundances of the different photofragment products from these two molecules are the same it implies that the dissociation dynamics is similar. Allene dissociates on the ground state surface after undergoing an internal conversion via a seam of crossing.³ There must be a place on the excited surface of propyne where it can also undergo internal conversion after rearrangement via this same seam of crossing. Direct dissociation from the excited state surface of propyne is in competition with this internal conversion. When allene is photolyzed at 193 nm, it produces C_3H_2 , and some of these radicals are photolyzed to produce C_3 .² The rotational distribution of 000 and 010 bands of C_3 produced in the photolysis of propyne is similar

^{a)}Author to whom correspondence should be addressed.

^{b)}Also at Chemistry Department, National Taiwan University, Taipei 106, Taiwan, R.O.C.

^{c)}Also at Department of Chemistry, University of California, Davis, California, 95616.

to the distribution observed from allene, but much less intense. It has been suggested that the same intermediate is produced in both cases through the same seam of crossing. Therefore, at least some of the excited propyne molecules arrive on the ground state surface. It has been suggested that about 10% of the excited propyne molecules undergo internal conversion to the highly vibrationally excited regions of the S_0 ground state of allene.² Thus, one of the goals of the present work was to discover whether the photodissociation channels in allene and propyne might be similar.

There have been other studies of the photodissociation of propyne. One of these is not photodissociation at all, but the Hg photosensitization reaction at 253.7 nm by Kebarle.⁵ This type of study can only populate the excited vibrational state in the ground potential or the first triplet state, since there is not enough energy to excite the first singlet state. They found that the primary process was H atom elimination, and this atom must come from the methyl end of the molecule because there is not enough energy to dissociate the hydrogen atom from the acetylene end of the molecule. Photolysis studies at 206 nm produce as the main products 1,5-hexadiyne, propylene, hydrogen, and acetylene, indicating there is some C–C bond rupture either via primary or secondary reactions.⁶ Theoretical calculations suggested that this may be the result of the lengthening and weakening of the C–H bond on the acetylene part of the molecule in the excited state.⁴ Stief and co-workers have studied the photodissociation of propyne at low pressures at 147.0 and 123.6 nm using deuterated isotope and product analysis.^{7,8} At 147.0 nm, they suggested that the reaction mechanisms are dominated by elimination of atomic hydrogen and molecular hydrogen.⁷ At 123.6 nm, they report that products of photodissociation occur exclusively via the molecular hydrogen elimination.

In the present paper, the results of UV photolysis studies of allene and propyne in molecular beams at 193 nm are reported. Laser VUV ionization is used to ionize the fragments, and TOF mass spectrometry was used to detect the nascent heavy photofragments.

EXPERIMENT

The essential elements of the apparatus consist of a pulsed nozzle, a time-of-flight mass spectrometer, a UV photolysis laser beam, and a VUV probe laser beam. The molecular beam, flight axis, and the VUV laser beam were oriented so that they were orthogonal to each other. The photolysis laser beam was in the same plane formed by the molecular beam and the VUV laser beam but it was at an angle of 15 deg relative to the VUV beam.

Allene was purchased from Fluka and mixed with He to form an 8% mixture. A similar mixture of 8% propyne in He was also made, but the propyne was purchased from Lancaster. Adiabatic expansion through a General Valve pulsed nozzle cools the seed molecules of allene or propyne. The stagnation pressure was kept at 800 Torr by using a pressure regulator. After skimming by two 1-mm diameter conical skimmers, the beam was entered into the photodissociation/ionization region of the time-of-flight mass spectrometer, 10 cm downstream from the nozzle. A pulse of 28-ns duration,

193-nm laser beam dissociates the cooled molecules. Photofragments were ionized by a pulsed VUV laser beam with a pulse duration of ~4 ns. The time delay between the UV photolysis laser beam and VUV probe beam was about 1 μ s. Ions that were formed in the interaction region were accelerated in a Wiley-McClaren-type double electrostatic field to 1.9 kV, and directed into an 80-cm long field-free flight tube. A chevron microchannel plate (MCP) detector was used to detect these ions. After amplification of the signal by a fast preamplifier, the mass spectrum was recorded with a digital oscilloscope and multichannel scalar (MCS) ion counter. The pressure during operation increased to 7×10^{-5} and 2×10^{-7} Torr in the source and ionization chambers, respectively.

The UV photolysis laser beam was obtained from a Lambda Physik Compex excimer laser (193 nm). The size of the *unfocused* UV photolysis laser beam was determined by a 2.5-mm iris. The UV laser beam entered the reaction chamber after passing through the iris and a CaF₂ entrance window. This beam exits the apparatus through a second CaF₂ window after passing through the molecular beam. The energy of the UV laser beam was monitored with a pyroelectric detector on the atmospheric side of the CaF₂ exit window. By this time, the diameter of the photolysis laser beam has diverged to 3.3 mm. Very low photolysis energies between 0.02 and 0.55 mJ per laser pulse were used at each of the photolysis wavelengths to insure that multiphoton and secondary photodissociation were minimized.

The VUV laser beam was generated by tripling the third harmonic of a *Q*-switched Nd-YAG laser in a phase matched Xe gas cell. The VUV and the third harmonic laser beams pass through a vacuum monochromator used in the first order where they are separated. A concave 1200 l/mm grating with a 98.5-cm radius is used in the monochromator for this separation. With this arrangement, only the VUV laser beam is sent to the ionization region of the time-of-flight mass spectrometer. The distances were set in such a way that the focal point of the VUV laser beam crosses the molecular beam 88 cm away from the grating.

The concentrations of the clusters in the molecular beam were checked by using the VUV laser beam to ionize the species in the beam when the UV photolysis laser beam is not present. Dimers and dimer fragments are observed in the TOF spectrum when the delay time between the pulsed valve and the laser is adjusted so the ionization laser arrives in the interaction region when the beam density is at a maximum. This is illustrated in Fig. 1(a) for allene. If, on the other hand, the ionization laser arrives on the leading edge of the pulsed molecular beam, Fig. 1(b) shows that almost no clusters are observed. All of the experiments that we report here were obtained using a delay to minimize interference from clusters. At the delay time we used, the intensity ratio between the mass of monomer and all masses higher than monomer is larger than 1000. Thus, contributions from cluster photolysis can be neglected.

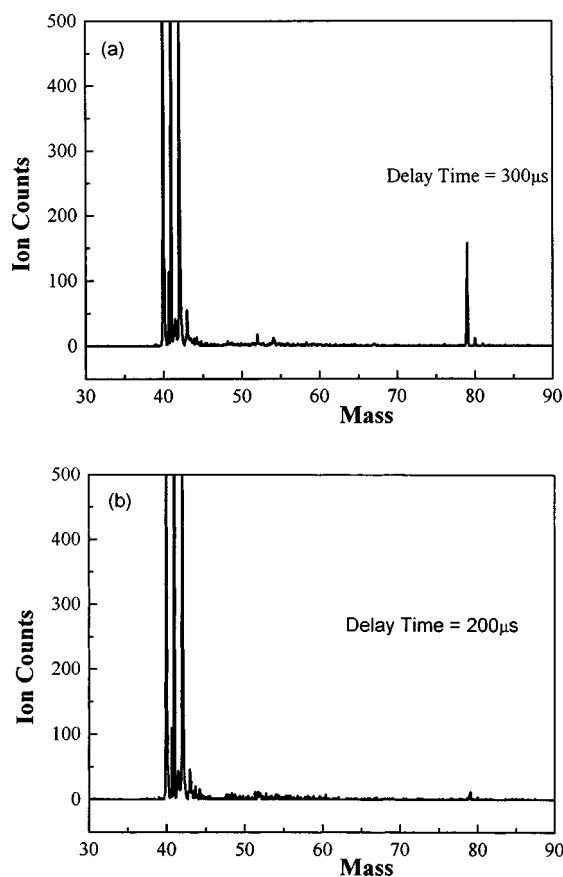


FIG. 1. The delay time between the pulsed valve and the laser is adjusted so the ionization laser arrives on (a) the center, (b) the leading edge of the pulsed molecular beam. The peaks at mass=41–45 are due to the ringing effect from the saturated signal at mass 40.

RESULTS AND DISCUSSION

Allene

Allene was photolyzed at 193 nm and ion masses at 14, 37, 38, and 39 were observed in the TOF spectra. Typical TOF spectra obtained at 193 nm are shown in Fig. 2(a). This spectrum shows peaks at masses 39, 38, 37, and 14. Power dependence measurements show that the mass 37 peak was due to multiphoton dissociation by the UV laser. The energy of the VUV photons used for ionizing the fragments was only 10.49 eV. Table I indicated that it is not high enough to produce CH_2 ions from larger fragments by dissociative ionization with one VUV photon.¹⁶ One of the isomer ions at $m/e = 38$, HC_3H^+ , could be produced by dissociation ionization of $\text{H}_2\text{C}_3\text{H}$ at 193 nm. However, the total photon energy (193+118 nm) is only 2.3 kcal/mol larger than the thermodynamic threshold. Reducing the total photon energy to below the thermodynamic threshold by changing the UV photon energy from 193 to 211 nm shows that the ratio of $m = 38/m = 39$ only changes from 0.07 to 0.06, which is within experimental error. Thus, $m/e = 38$ ions are not likely to be produced by the dissociation ionization of $m = 39$ fragments. The VUV laser fluence is about 10^{10} photon/pulse with pulse duration of 4 ns focused to about a 100- μm diameter spot. So, it is unlikely to produce fragment ions by multiphoton

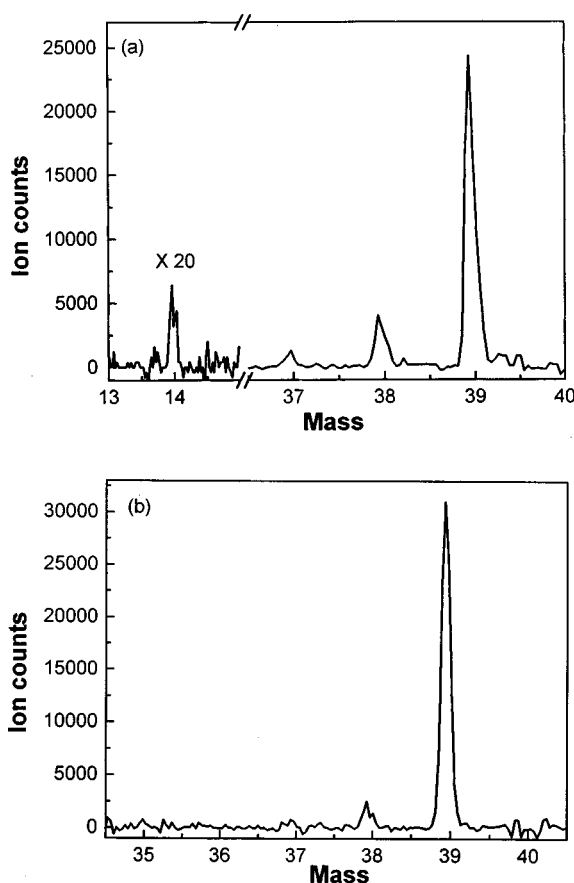
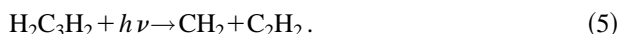


FIG. 2. The photofragment time-of-flight mass spectrum of (a) allene, (b) propyne. The noises at nonintegral masses are due to multiphoton ionization by the photolysis laser beam.

ionization. We therefore conclude that the observed products indicate that reactions 1, 2, and 5 are the three primary processes occurring in the photolysis of allene,



Acetylene must be produced by reaction 5 because the only other possible product is vinylidene (H_2CC). The lowest energy spin-allowed reaction to produce methylene and vinylidene is $\text{CH}_2(a^1\text{A}_1) + \text{H}_2\text{C}_2(X^1\text{A}_1)$, which requires 157.1 kcal/mol. This is 8.9 kcal/mol higher than the energy of a 193-nm photon, so it is energetically impossible for one photon. The H, H_2 , and C_2H_2 are not observed in the TOF spectra because their ionization potentials are higher than the energy of a 118.2-nm photon.¹⁶

The largest signal in the present experiments is mass 39, which corresponds to the C_3H_3^+ ion. This agrees with the earlier results from photofragment spectroscopy.¹ The mass 39 power dependence shows that it is produced by one UV photon. The signal of mass 39 was used to normalize the yield of the C_3H_2 and CH_2 channels. By doing this one can take into account day-to-day differences in alignment of the ionizing and photolysis lasers with respect to the molecular beam. The observed ratio can be converted to a relative yield when the relative photoionization cross sections are known. Figure 3(a) is a plot of the relative signal size as a function of the photolysis laser power. The relative intensity of mass 14 to mass 39 was independent of laser power. This indicates

TABLE I. The heat of reaction of observed ions produced from large fragments by dissociative ionization. All energies in kcal/mol. The observed ions are not thermodynamically allowed to be produced by dissociative ionization of large fragments due to the energies of heat of reactions larger than the total energy of UV (193 or 211 nm) and VUV (118.2 nm) photon energies.

allene	$E(193 \text{ nm} + 118 \text{ nm})$	$E(211 \text{ nm} + 118 \text{ nm})$	ΔH	Ref.
$\text{H}_2\text{C}_3\text{H}_2 + h\nu_{\text{uv}} \rightarrow \text{H}_2\text{C}_3\text{H} + \text{H} + h\nu_{\text{vuv}} \rightarrow \text{C}_3\text{H}_2^+ + 2\text{H}$	390.4	378.0	425.2	4,16
$\text{H}_2\text{C}_3\text{H}_2 + h\nu_{\text{uv}} \rightarrow \text{H}_2\text{C}_3\text{H} + \text{H} + h\nu_{\text{vuv}} \rightarrow \text{HC}_3\text{H}^+ + 2\text{H}$	390.4	378.0	388.1	4,16
$\text{H}_2\text{C}_3\text{H}_2 + h\nu_{\text{uv}} \rightarrow \text{H}_2\text{C}_3\text{H} + \text{H} + h\nu_{\text{vuv}} \rightarrow \text{CH}_2^+ + \text{C}_2\text{H} + \text{H}$	390.4	378.0	470.5	4,16
$\text{H}_2\text{C}_3\text{H}_2 + h\nu_{\text{uv}} \rightarrow \text{C}_3\text{H}_2 + \text{H}_2 + h\nu_{\text{vuv}} \rightarrow \text{CH}_2^+ + \text{C}_2 + \text{H}_2$	390.4	378.0	486.9	4,16
$\text{H}_2\text{C}_3\text{H}_2 + h\nu_{\text{uv}} \rightarrow \text{HC}_3\text{H} + \text{H}_2 + h\nu_{\text{vuv}} \rightarrow \text{CH}_2^+ + \text{C}_2 + \text{H}_2$	390.4	378.0	486.9	4,16

that both of them have the same laser power dependence. A similar plot for the C_3H_2^+ to C_3H_3^+ yields shows that the C_3H_2^+ ion has a higher power dependence than the CH_2^+ ion. This indicates that the signal contains a multiphoton component, which is present even at the low unfocused 193-nm laser fluence that we have used. The multiphoton component was estimated to be less than 10% of the signal at the highest UV laser energies which were used. The laser fluence employed in these experiments was between 2 and 8 mJ/cm^2 pulse. This is the lowest fluence per pulse that has been used in any of the experiments on allene. In fact, we found the

ratio $m=38/m=39$ signal increased to 0.3 when the UV laser fluence increased to $80 \text{ mJ}/\text{cm}^2$. The earlier photofragment spectroscopy experiments showed that the peak of internal energy of the C_3H_3 fragment was 56 kcal/mol.¹ The present experiments show that this internal energy really increases the probability for absorption of a secondary photon.

A linear extrapolation of the $[\text{C}_3\text{H}_2^+]/[\text{C}_3\text{H}_3^+]$ to zero laser power indicates the relative signal size is 0.07. This is smaller by a factor of 1.5 than the earlier estimate of 0.12 for the relative quantum yield.¹ It is actually surprising that the present relative signal size is so close to the previous value for the relative quantum yield. The detection efficiencies of mass 38 and 39 should be similar because the masses and velocities are almost the same. The relative photoionization cross sections must also be similar to explain the present results. The ionization potentials of C_3H_3 and C_3H_2 are 8.67 and 10.43 eV, respectively. The latter value is very close to the energy of the ionizing photon that is 10.49 eV. The internal energy in the C_3H_2 radicals (34 kcal/mol)¹ must greatly enhance the ionization cross section at 10.49 eV, which results in similar cross sections for C_3H_3 and C_3H_2 .

The presence of signal at mass 14 indicates the production of methylene as a previously unobserved primary product via reaction 5. The relative intensity of this low mass channel at zero laser power is 0.01, which is small relative to the other channel. This explains why it has not been previously observed, because of the difficulty in determining the presence of photofragments at these low masses using photofragment spectroscopy.

Propyne

A typical TOF spectrum of the ions of photofragments produced in the photolysis of propyne at 193 nm is shown in Fig. 2(b). Two photofragments, at masses 39 and 38, are observed in this spectrum. The power dependence of mass 39 shows that it is produced by one UV photon. The relative ion intensities of the C_3H_2 and the C_3H_3 fragments are plotted in Fig. 3(b) as a function of the laser fluence. The error bars of the ratio $m=38/m=39$ at low photolysis fluence are relatively large. This is because the signal of $m=39$ becomes small at low photolysis fluence, but the background noise at $m=38$ is not reduced as much as the $m=39$ signal, which results in the larger error bar at low photolysis fluence. However, the signal of $m=38$ after the subtraction of the background converges to zero at low photolysis fluence. The

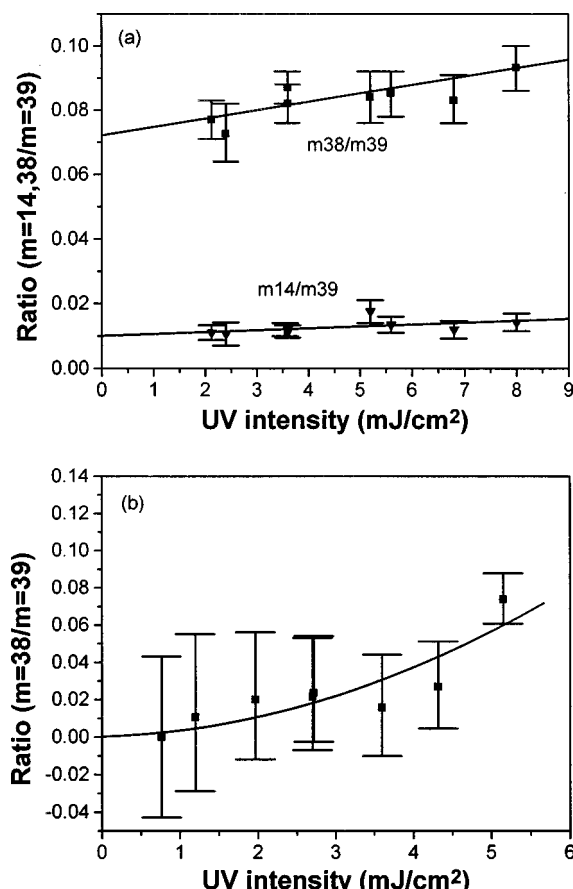


FIG. 3. (a) The plot of allene photofragment ratios mass=14/mass=39 and mass=38/mass=39 as a function of UV laser power. Solid lines represent the fit of the function $Y = A + B \times X$, in which $A = 0.010$, $B = 5.8 \times 10^{-4}$ for mass=14 and $A = 0.072$, $B = 0.0024$ for mass=38. (b) The plot of propyne photofragment ratio mass=38/mass=39 as a function of UV laser power. The solid curve represents the fit of the function $Y = A + B \times X + C \times X^2$, in which $A = 0.003$, $B = 9.1 \times 10^{-4}$, $C = 0.0024$.

power dependence of the $C_3H_2^+$ signal shows that most of the C_3H_2 results from two UV photons, even when the UV laser fluence is as low as 5 mJ/cm². At very low fluence, a small amount of C_3H_2 may be produced by one photon photolysis, via



The amount of C_3H_2 produced at zero fluence was not larger than 0.5% of C_3H_3 . The difference between the $m=38/m=39$ ratio in allene and propyne suggests that the photodissociation mechanism is different for these two geometrical isomers. Unequal ratios of $m=38/m=39$ also imply that dissociation occurs before complete isomerization for these two molecules. If there is any isomerization of propyne to allene, it would be less than 7% of the excited molecules.

A very small peak in the TOF spectra is observed at mass 14, which would correspond to reaction (4), which was originally proposed by Okabe.¹⁰ This peak was so small that it could not be further analyzed. It does show that if both of these products are formed via dissociation on the ground state surface, the initial geometry of the reactant affects the branching ratio. This further implies that redistribution of energy and isomerization do not occur as fast as dissociation.

The results that have been obtained can now be compared with the theoretical calculations of the ground and excited state potential surfaces of allene and propyne.^{3,4,11–13} The calculations on the excited states of allene in the 193-nm region suggest that the initial excitation is to a state allowed by vibronic interaction. This state is planar and thus this excitation imparts an internal rotation to the CH_2 group in the excited state.³ The photoexcitation process is followed by rapid internal conversion of the S_1 state to the S_0 state via a seam of crossing. Once the molecule is on the ground state surface there are a variety of options available to it. It can undergo H and H_2 elimination,^{3,4} isomerization to propyne, cyclopropene, propenylidene, and trans-vinylmethylene, as well as fragmentation to methylene and acetylene.^{11–14} The highest barrier to isomerization between all of the species on the ground state surface is 66.1 kcal/mol, which is smaller than the 148 kcal/mol of energy available after internal conversion. By comparison of the theoretical potential energy surfaces and the fragment translational energy of allene,^{1,3,4} one can conclude that H and H_2 eliminations in allene can be explained by dissociation on the ground state surface.

The carbon–carbon bond rupture channels in allene have not yet been theoretically investigated but it is clear that they are different in these two molecules. Carbon–carbon bond rupture in allene will probably have a barrier because of the H atom migration. The earlier theoretical calculations suggest that H migration can lead to vinylmethylene or cyclopropene followed by a ring closing step, which could decompose to form $CH_2 + C_2H_2$.¹² There is not enough energy at 193 nm to form the only other spin-allowed channel, i.e., $CH_2(a^1A_1) + H_2C_2(X^1A_1)$, because the threshold energy is 157.1 kcal/mol. Calculations are in progress to determine the height of this barrier and the nature of the transition state.

Theoretical calculations of propyne by Mebel *et al.*⁴ suggested that the apparent preference for elimination of an H atom with a bond strength of 130.5 kcal/mol over one with

an energy of 88.7 kcal/mol could be rationalized in terms of the structure $S_2(cis), 2^1A'$ state. In this state, the acetylenic C–H bond distance increases 1.131 Å and there are no barriers to the elimination of this H atom. The theoretical calculations also show that there are two molecular H_2 elimination channels on the ground state surface, namely, 1, 1 and 1,3 elimination. If the excited state surfaces cross with the ground state surface, internal conversion of the electronically excited propyne to the ground state surface should compete with dissociation on the excited surface. The present studies show that most of the excited propyne molecules dissociate through the H atom elimination channel. The relatively small amount of H_2 elimination from propyne compared to the amount from allene explains why the C_3 yield from propyne is smaller than the yield from allene, even though the propyne absorption cross section at 193 nm is larger than the allene cross section.

CONCLUSIONS

VUV laser photoionization has been used to determine the heavy fragments produced in the laser photodissociation of allene and propyne. These studies have been performed in a molecular beam under collisionless conditions. It has been shown that very low laser energies have to be used to insure that the products that are observed are not formed by secondary photolysis. The results of the studies indicate that the major primary process in both allene and propyne is H elimination. In addition to H atom elimination, two other channels are observed in allene, namely 1,1 hydrogen molecule elimination channel and C–C bond rupture. The channel that produces CH_2 observed in allene must involve a more complicated rearrangement reaction. The different ratio of various dissociation channels in allene and propyne suggests that the dissociation mechanisms of these two molecules are different. The geometry on the excited state surface can affect the relative value of internal conversion and direct dissociation, and the isomerization between these two molecules is not as fast as the dissociation. It is likely that H atom production in propyne occurs in the excited state, but in allene it occurs on the ground state surface. The H and H_2 signal ratios in allene are similar to the relative yields observed in the earlier photofragment spectroscopy studies. This suggests that the signal sizes are a fair measure of the relative concentrations of the heavy fragments.

ACKNOWLEDGMENTS

This project is supported by the China Petroleum Research Corporation. J.D.H. and Y.T.C. also acknowledge the support of the National Science Council of R.O.C. under Grant No. NSC88-2113-M-001-031, and W.M.I. the support of the Alexander Von Humboldt Foundation and NASA's Planetary Atmospheres Program under Grant No. NAG5-4711.

¹ W. M. Jackson, Deon S. Anex, R. E. Continetti, B. A. Balko, and Y. T. Lee, *J. Chem. Phys.* **95**, 7327 (1991).

² X. Song, Y. Bao, R. S. Urdahl, J. N. Gosine, and W. M. Jackson, *Chem. Phys. Lett.* **217**, 216 (1994).

- ³ W. M. Jackson, A. M. Mebel, S. H. Lin, and Y. T. Lee, *J. Phys. Chem.* **101**, 6638 (1997).
- ⁴ A. M. Mebel, W. M. Jackson, A. H. H. Chang, and S. H. Lin, *J. Am. Chem. Soc.* **120**, 5751 (1998); Q. Cui, K. Morokuma, and J. F. Stanton, *Chem. Phys. Lett.* **263**, 46 (1996).
- ⁵ P. Kebarle, *J. Chem. Phys.* **39**, 2218 (1963).
- ⁶ A. Galli, P. Harteck, and R. R. Reeves Jr., *J. Phys. Chem.* **71**, 2919 (1967).
- ⁷ L. J. Stief, V. J. DeCarlo, and W. A. Payne, *J. Chem. Phys.* **54**, 1913 (1971).
- ⁸ W. A. Payne and L. J. J. Stief, *Chem. Phys.* **56**, 3333 (1972).
- ⁹ S. Satyapal and R. Bersohn, *J. Phys. Chem.* **95**, 8004 (1991).
- ¹⁰ K. Seki and H. Okabe, *J. Phys. Chem.* **96**, 3345 (1992).
- ¹¹ N. Honjou, J. Pacansky, and M. Yoshimine, *J. Am. Chem. Soc.* **107**, 5332 (1985).
- ¹² M. Yoshimine, J. Pacansky, and N. Honjou, *J. Am. Chem. Soc.* **111**, 2785 (1989).
- ¹³ M. Yoshimine, J. Pacansky, and N. Honjou, *J. Am. Chem. Soc.* **111**, 4198 (1989).
- ¹⁴ L. M. Lesiecki, K. W. Hicks, A. Orenstein, and W. A. Guillory, *Chem. Phys. Lett.* **71**, 72 (1980).
- ¹⁵ A. Lifshitz, M. Frenklach, and A. Burcat, *J. Phys. Chem.* **79**, 1148 (1975).
- ¹⁶ The National Institute of Standards and Technology (NIST) Chemistry Webbook: <http://webbook.nist.gov/chemistry/>